

The Statistics of the Prompt-to-Afterglow GRB Flux Ratios and the Supercritical Pile GRB Model

D. Kazanas^{*†}

NASA/GSFC, Code 663, Greenbelt, MD 20771

E-mail: Demos.Kazanas@nasa.gov

J. L. Racusin

NASA/GSFC, Code 661, Greenbelt, MD 20771

E-mail: judith.racusin@nasa.gov

J. Sultana

Mathematics Department, Faculty of Science, University of Malta, Msida MSD2080 Malta

E-mail: joseph.sultana@um.edu.mt

A. Mastichiadis

Department of Physics, University of Athens, Panepistimiopolis, GR 15783, Zografos, Greece

E-mail: amastich@physics.uoa.gr

We present the statistics of the ratio, R , between the prompt and afterglow "plateau" fluxes of GRB. This we define as the ratio between the mean prompt energy flux in the *Swift* BAT and the *Swift* XRT, immediately following the steep transition between these two states and the beginning of the afterglow stage referred to as the "plateau". Like the distribution of other GRB observables, the histogram of R is close to log-normal, with maximum at $R = R_m \simeq 2,000$, FWHM of about 2 decades and with the entire distribution spanning about 6 decades in the value of R . We note that the peak of the distribution is close to the proton-to-electron mass ratio ($R_m \simeq m_p/m_e = 1836$), as proposed by us earlier, on the basis of a specific model for the conversion of the GRB blast wave kinetic energy into radiation, before any similar analysis were made. It therefore appears that, in addition to the values of the energy of peak luminosity $E_{pk} \sim m_e c^2$, GRB present us with one more quantity with an apparently characteristic value. The fact that the values of both these quantities (i.e. E_{pk} and R) comply with those implied by the same specific model devised to account for an altogether different issue, namely the efficient conversion of the GRB blast wave kinetic energy into radiation, argues favorably for its underlying assumptions.

10th INTEGRAL Workshop: "A Synergistic View of the High Energy Sky" - Integral2014,

15-19 September 2014

Annapolis, MD, USA

*Speaker.

†Work supported by *Fermi* GI funds

1. Introduction

The nature of Gamma-Ray Bursts (GRB), short duration ($\sim 10^{-2} - 10^2$ s), γ -ray emission events at cosmological distances, remains enigmatic despite much observational and theoretical progress over the past twenty five years. Furthermore, they appear to present us with novel puzzles each time improvements in instrumentation allow for significant improvement in measuring their properties. One such example is the shape of their afterglow light curves, which the *Swift* observations showed to be vastly different from those predicted by the early theoretical considerations, the subject of the present note.

The cosmological origin of GRB was essentially confirmed with the discovery of their afterglows. This set the redshifts of their host galaxies, determined their distances to be cosmological and their luminosities in the range of $\sim 10^{50} - 10^{54}$ erg/s. Their implied high specific intensities, then, argued for emission by the plasma of relativistic blast waves (RBW) of Lorentz factor (LF) $\Gamma \gtrsim 200$ [20], a fundamental tenet of the physics of these events. However, while the association of GRB with RBW is undisputable, there are still serious gaps in our fundamental understanding of their radiation emission: Ignoring for the moment the origin of flows with $\Gamma \gtrsim 200$, a RBW is an inertial agent, distributing the postshock energy in proportion to the swept particles' mass. So, the electrons, the only particles that can radiate efficiently, carry only a fraction ($\eta \sim 1/2000 \sim m_e/m_p$) of the shock's energy. Because such a small efficiency would lead to unrealistically large GRB energies and luminosities, the issue is resolved by *assuming* that the protons and electrons share equally the postshock energy. Another open issue associated with the GRB prompt stage is the rather limited range of the energy of peak luminosity, $E_{\text{pk}} \sim 0.3$ MeV (extending on occasions to a few MeV), intriguingly close to the electron rest mass on the Earth frame, but not on the GRB rest frame, considering the large Lorentz factors of their blast waves. This characteristic energy is *the* defining attribute of the GRB prompt emission since the energy of peak luminosity declines very fast as GRB develop in time and enter their, less variable, afterglow stage.

Afterglows have been considered to be, ever since their discovery, a distinct and separate phase of the GRB phenomenon. However, there does not appear to be a formal criterion that determines the transition from the prompt to the afterglow GRB phase. Operationally, the prompt phase ends when the GRB flux drops below the *Swift*-BAT sensitivity threshold. On theoretical grounds, it is generally considered that the prompt GRB phase terminates when the RBW reaches its deceleration radius R_D , since, beyond this point its LF begins to decrease (R_D is the radius at which the RBW has swept-up mass-energy $Mc^2 \simeq m_p c^2 n R_D^3 \simeq E/\Gamma^2$; E is total energy of the RBW, n the circumburst density - assumed to be constant - and Γ its Lorentz factor). The decrease of the GRB Lorentz factor for $R > R_D$ ($\Gamma \propto R^{-3/2}$ for adiabatic evolution in a uniform density medium) leads to a decrease in the GRB flux and to the energy of its peak luminosity, E_{pk} , which moves out of the *Swift*-BAT range. The afterglow emission, just as that of the prompt phase, is considered in most models to be synchrotron radiation by shock accelerated electrons, in rough equipartition with the protons of the postshock region. Under these assumptions, one can compute for the GRB afterglow stage the resulting spectrum and its time evolution. The computation of the GRB X-ray flux evolution in time was first performed for spherically symmetric outflows in [21] and in [22] for jet-like outflows, assuming the spectrum of electrons injected at the shock to be $dN/dE \propto E^{-p}$, $p \gtrsim 2$. The model X-ray light curves were, then, shown to be power laws in time, $F_X \propto t^{-\alpha}$, $\alpha \gtrsim 1$, with a smooth

transition between the prompt and afterglow GRB stages, in broad agreement with the sparsely sampled afterglow light curves of the pre-*Swift* era.

The launch of *Swift* and its ability to follow closely the evolution of GRBs from their prompt (γ -ray emitting) to the afterglow (X-ray emitting) stages provided yet another set of unexpected, puzzling facts, grossly inconsistent with expectations based on the models described above [27, 16, 30, 1]: Instead of the predicted decrease of their X-ray flux as $L_x \propto t^{-\alpha}$, $\alpha \gtrsim 1$, the decrease is much steeper ($\alpha \sim 3 - 6$), followed either (i) by a much shallower section (referred to as the "plateau") ($\alpha \sim 0$), which is succeeded for $t > T_{\text{brk}} \sim 10^3 - 10^5$ sec by a decline of $\alpha \simeq 1$ or (ii) by a more conventional decline ($\alpha \simeq 1$) (these light curves exhibit also occasionally large amplitude flares which we will not discuss at present).

The unexpected afterglow light curves prompted a number of accounts of their behavior within the standard GRB model [see §3.1.1 of [31] and references therein]. The most conventional such account is that the steep decay represents high latitude (with respect to the observer's line of sight) emission; while steeper ($\alpha \simeq 2$) than the law derived in [21], this is still less steep than most commonly observed and certainly at great odds with declines as steep as t^{-6} . Alternative explanations attribute this to the form of the underlying electron distribution [9, 6] while [17], by adjusting the maximum energy γ_{max} of the electron distribution, interpret the steep decline segment as synchrotron emission by the fast cooling, high energy cutoff of the electron distribution function and the "plateau" segment to inverse Compton by its more slowly varying low energy section.

The plateau segment, because it follows that of the very steep flux decline, gives the impression of a distinct and completely separate emission from that of the GRB prompt phase. For this reason, it was proposed (not unreasonably) that it indicates the emergence of an additional injection of energy by the GRB central source, separate from that producing the shorter but brighter prompt emission [29]. Along these lines, the authors of [7] even specify this additional injection to be due to the propeller effect of an underlying magnetar which presumably powers the entire burst. Anyway, these attempts to account for the behavior of the GRB afterglow light curves were devised to model these specific features, without any reference to, or consideration of, the broader properties of the entire burst. Alternatively, several treatments have focused instead on just the properties of the plateau phase itself, leaving its origin unspecified. Of these we mention those of [10] and [24] who, by fitting the spectro-temporal evolution of the afterglow plateau segment of several GRB, conclude that this emission takes place *before* the RBW has reached its deceleration radius R_b .

2. Afterglows in the Supercritical Pile Model (SPM)

An altogether different approach to the afterglow evolution has been that of [25]. This is different in that the afterglow evolution, including all its details, is produced as an integral part of the evolution of the entire burst, beginning with the accelerating phase of the RBW and continuing with its dissipation and prompt emission, including also the correct value of the energy of the GRB prompt phase emission, E_{pk} . The central notion of this model is a radiative instability that converts the relativistic proton energy behind the RBW forward shock to e^+e^- -pairs through the $p\gamma \rightarrow pe^+e^-$ reaction; the pairs then produce more synchrotron photons, which produce more pairs and so on [8, 11, 12, 13]. This instability requires that the column of relativistic protons in the postshock region be larger than a critical value, in direct analogy with a supercritical nuclear

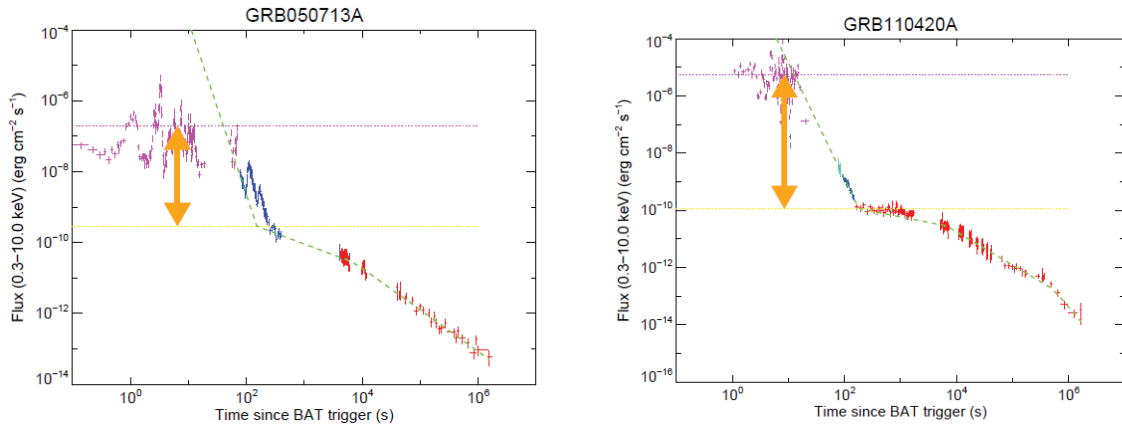


Figure 1: (a) The prompt to afterglow light curves of the gamma ray bursts indicated on the figure. The prompt, transition and afterglow plateau stages are apparent. The two dotted lines represent the mean prompt flux (top, purple line) and afterglow (bottom, red line) fluxes involved in computing the flux ratios of these two states.

pile (hence the nomenclature Supercritical Pile Model or SPM); put simply, one cannot accumulate arbitrarily large columns of relativistic protons for the same reason that one cannot accumulate arbitrarily large amounts of U^{235} : They explode! However, besides this condition on the proton column, the instability imposes a kinematic constraint on the synchrotron photon energy because the synchrotron photons emitted by the e^+e^- -pairs must be able to pair-produce in collisions with the protons. This effectively requires the RBW Lorentz factor to be larger than a critical value, Γ_c , given by the condition $\Gamma_c^5 b \simeq 1$, a demand imposed by the kinematic threshold of the above reaction ($b = B/B_{cr}$ is the postshock value of the GRB magnetic field with $B_{cr} = 4.4 \times 10^{13}$ G the value of the critical magnetic field). Incidentally, the energy of peak emission of the prompt phase of this model, *on the Earth frame*, is also (in units of $m_e c^2$) $E_{pk} \simeq \Gamma^5 b \simeq 1$, so in this model, the observed characteristic value of E_{pk} reflects simply the threshold energy of pair production on the GRB frame.

Another crucial element of this model is the upstream scattering of the RBW synchrotron radiation and its re-interception by it. As noted in [12, 13] and more specifically in [25], this process induces a radiation reaction on the RBW and causes a (relatively) small ($\sim 30\% - 50\%$) reduction of its Lorentz factor over a radius $\Delta R \ll R$. Even though small, this reduction is important because it pushes Γ below the threshold value Γ_c , thus arresting the transfer of energy from the RBW relativistic protons into e^+e^- -pairs. As noted in [25] this event should result in an abrupt reduction of the RBW radiative flux (producing the observed steep decline), thereby defining the end of the prompt GRB phase and the beginning of the afterglow. The authors of [25] estimated the reduction in flux to be by a factor roughly equal to the proton-to-electron mass ratio, i.e. by $\sim m_p/m_e \simeq 2000$, since the emitted radiation now comes from the cooling of *only the electrons* being swept-up by the RBW. Furthermore, the radius at which this small, sharp reduction in Γ takes place is generally smaller than R_D . Because an RBW expands with constant Γ until it amasses enough inertia to begin its decline at $R > R_D$, it will continue to do so at its new, smaller Γ , and with the GRB now being in its afterglow stage. Then, depending on the rate of decrease of the RBW magnetic field with radius or the density profile of the ambient medium [24], the ensuing synchrotron (or Compton) emission could be constant, decreasing slightly or even increasing with time, producing thus the

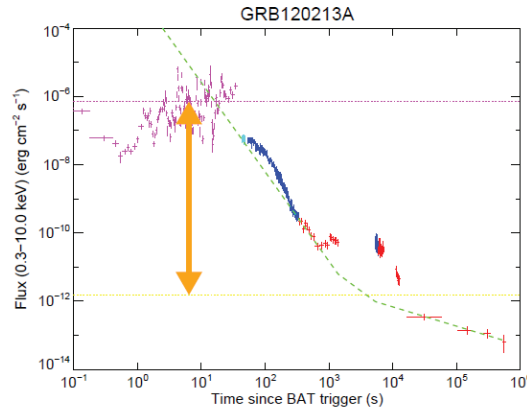


Figure 2: Same as in figure 1 but for GRB 120213A. The two horizontal lines indicate the flux levels that our algorithm has chosen in computing the ratio R . Eye inspection indicates that a more reasonable value is $\sim 10^4$, considering that there appears to be a plateau beginning at $t \simeq 10^3$ sec.

afterglow plateau emission. Finally, beyond the deceleration radius, which is reached at time T_{brk} (a time associated within the model with R_D) a more conventional decrease in afterglow flux ensues, consistent with the standard analyses[21].

Motivated by the specific value of the flux ratio, R , between the prompt GRB and the afterglow plateau stages implied by the model put forward in [25], we have compiled and present in this note the distribution of R obtained from a large number of GRB afterglows of the *Swift-XRT* repository [1, 2]. This is presented in the next section. Along with this we also present a correlation between L_{iso} , the peak isotropic luminosity of the prompt emission and the afterglow X-ray luminosity L_X at time $t = T_{\text{brk}}$, the time the X-ray afterglow resumes its more conventional decay. We finish in §4 with our conclusions and some discussion.

3. The Prompt-to-Afterglow Flux Ratios

Following the arguments presented above, we have searched the *Swift* data base and compiled the ratios, R , between the prompt and afterglow GRB fluxes. We have used fits to the average BAT light curves obtained from the *Swift-XRT* repository Burst Analyzer [2] extrapolated down to the 0.3–10 keV band from fits to the XRT, as described in [18, 19], to extract the flux at the transition between steep decline and plateau in the afterglows demonstrating that form. In figures 1a,b and 2 we present three specific cases of GRB transitions from the prompt to the afterglow stages with a variety of post transition behaviors. The fast decline exponents range between $\alpha \simeq -3$ and $\alpha \simeq -6$, while their transition to $\alpha \simeq -1$ happens in all cases around $T_{\text{brk}} \simeq 10^4$ sec. The yellow arrows show the decrease in flux between the *geometric mean* of the highly variable prompt emission and the end of the steep decline phase.

These figures indicate that these transitions have peculiarities of their own. For example the decrease of GRB 050713A is by a factor $R \simeq 10^3$, smaller than the m_p/m_e ratio; however, in the other two GRB the decrease, as shown by the yellow arrows, is by factor 10^4 and 10^6 , one of them significantly larger than the m_p/m_e ratio. On the other hand this last case, namely of GRB 120213A, exhibits a rather peculiar two step transition; in the first step, the flux decreases by $\sim 10^4$

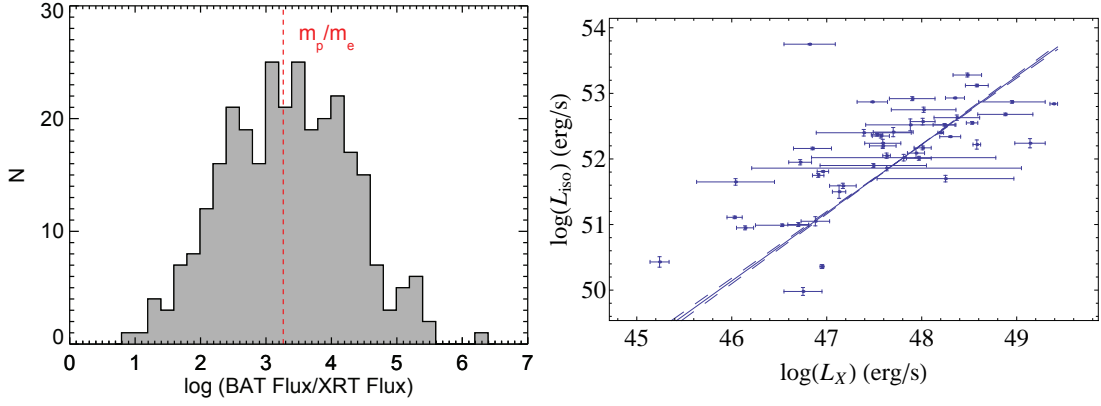


Figure 3: The histogram of the BAT to XRT flux ratio for a number of *Swift* GRB. The distribution shows clearly a preferred value for this ratio of order $\sim 10^3 - 10^4$. The vertical line shows also the proton to electron mass ratio m_p/m_e .

and it is followed by another one by an additional factor of 10^2 . The horizontal lines and the yellow arrow in Fig. 2 indicate the fluxes considered by the algorithm employed for extracting the afterglow parameters. This last case indicates that, besides applying a given algorithm, one may have to scrutinize each such transition individually.

From the point of view of the data available in search of correlations among GRB attributes, the one proposed in [25] and tested herein has the clear advantage that it involves only flux ratios rather than absolute values (whether luminosities, time lags or values of E_{pk}) as is the case with many of the GRB produced correlations (e.g. the Lag-Luminosity relation, the E_{pk} - E_{iso} , the $L_X - T_{brk}$. etc. correlations). As such, knowledge of the GRB redshift is not necessary, a fact that allows the compilation of a large number of bursts. The ratios of the prompt to afterglow fluxes were compiled from the *Swift*-XRT repository and spans the period between December 2004 and March 2014.

The main result of our analysis is given in Fig. 3a where we present a histogram of the logarithm of the BAT-to-XRT flux ratio, R , computed as described above along with a dashed vertical line that indicates the value of the m_p/m_e ratio. The distribution exhibits a broad maximum at almost precisely this value, indicating the presence of a characteristic ratio between the prompt and afterglow fluxes, as proposed in [25]. The R -distribution appears to be log-normal, though its precise shape is not easy to determine accurately. It spans 5-6 decades in R , with a FWHM of about 2 decades and a median value of $\log R$ essentially equal to that of $\log(m_p/m_e) \simeq 3.25$ and a slightly larger medium value ($\simeq 10^4$) in sufficient agreement with the suggestion of [25] to merit further consideration.

As mentioned above, a number of correlations has already been established between GRB prompt or afterglow emission characteristics, such as the Lag-Luminosity relation [14, 15, 23], the maximum prompt emission (isotropic) luminosity L_{iso} and the peak energy of the Band function E_p [23, 28] and the afterglow plateau X-ray luminosity L_X and the rest-frame plateau end-time T_{brk} , beyond which the afterglow resumes the standard decline [3, 4, 5]. In [26] we showed that the Lag-Luminosity of the prompt emission extrapolates into the $L_X - T_{brk}$ afterglow correlation, suggesting

the intimate connection of these phases, despite the apparent absence of continuity between them (however, there is a correlation between the two within the SPM). Motivated by this relation and the histogram of Fig. 3a, we bypass the time coordinate of the relation given in [26] and plot in Fig. 3b the maximum prompt isotropic luminosity L_{iso} vs. the X-ray luminosity of the afterglow plateau segment at the time T_{brk} . There appears to be a correlation between these quantities. A least squares fit gives the following relation between L_{iso} and L_X

$$\log L_{\text{iso}} = (4.04 \pm 0.10) + (1.04 \pm 0.02) \log L_X \quad (3.1)$$

with correlation coefficient $\rho = 0.69$. The ratio of these two quantities appears consistent with that shown in Fig. 3a. Given the difference in the choice of these samples and the slightly different properties they depict, they appear to be consistent with each other and the general premise of the prompt to afterglow luminosity ratios.

4. Discussion, Conclusions

Motivated by the considerations put forward in [25], based on the SPM of GRB dissipation, we have compiled the flux ratios between the prompt and the afterglow plateau stages of GRB to indicate that there is indeed a characteristic value for the ratio R of these two quantities. The important point to bear in mind is that this characteristic value for R , namely m_p/m_e , was proposed in [25] *before* the compilation of the histogram of Fig. 3a; as such, it constitutes a *prediction* of the model, one of the very few in the GRB field of study. A similar relation has also been found between slightly different quantities of these two GRB phases, shown in Fig. 3b, one that requires, however, knowledge of their redshifts.

One must note at this point that though there is a maximum in the distribution of fluxes near the value m_p/m_e , the histogram of Fig.3 has a finite width. Thus there are bursts with R values as large as 10^6 and as low as 10^2 . Figure 2 shows a burst with a particularly large value of this ratio. As argued earlier, one could assign to this burst a value smaller than that given by our algorithm, given the peculiar form of its afterglow. On the other hand, if one takes into account that the observed luminosity has a dependence on the Lorentz factor of the flow Γ as strong as Γ^4 , even a small reduction in Γ could increase the pre-to-post prompt emission fluxes to values larger than m_p/m_e . Values of $R < m_p/m_e$ would appear to be more problematic. An account of these values, put forward in [25], is that not all protons "are burnt" in prompt phase, thus reducing the flux of this stage. A different possibility is that in these cases, the original angle of the jet to the observer's line of sight, θ , is slightly larger than $1/\Gamma$, yielding a reduced relativistic boosting for the prompt emission; after the RBW radiation-reaction slowdown, the smaller value of Γ allows the observer's line of sight to "peer" directly into the (wider now) relativistic outflow, thereby reducing the ratio of the pre-to-post prompt emission fluxes. If this is the case, then the prompt emission of bursts with $R < m_p/m_e$ should be indicative of this situation, e.g. they should exhibit longer Lags, smaller E_{pk} , smaller L_{iso} , issues that could in principle be tested by an appropriate choice of a GRB sample. However, such considerations are beyond the scope of the present note.

References

- [1] Evans, P. A. et al. 2009, MNRAS, 397, 1177

- [2] Evans, P. A. et al. 2010, *A&A*, 519, A102
- [3] Dainotti, M. G., Cardone, V. F., & Capozziello, S. 2008, *MNRAS*, 391, L79
- [4] Dainotti, M. G., Willingale, R., Capozziello, S., Cardone, V. F., & Ostrowski, M. 2010, *ApJ*, 722, L215
- [5] Dainotti, M. G., Petrosian, V., Singal, J., & Ostrowski, M. 2013, *Apj*, 774, 157
- [6] Giannios, D., & Spitkovsky, A. 2009, *MNRAS*, 400, 330
- [7] Gompertz, B. P., O'Brien, P. T. & Wynn, G. A. 2014, *MNRAS*, 438, 240
- [8] Kazanas, D., Georganopoulos, M., & Mastichiadis, A. 2002, *ApJ*, 587, L18
- [9] Kazanas, D., Mastichiadis, A., & Georganopoulos, M. 2007, *ESASP* 622, 577 (also astro-ph/0612046)
- [10] Lei, H.-D., Wang, J.-Z., Lü, J. & Zou, Y.-C. 2011, *Chinese Physics Letters*, 28, 129801
- [11] Mastichiadis, A., & Kazanas, D. 2006, *ApJ*, 645, 416
- [12] Mastichiadis, A., & Kazanas, D. 2008, *Proc. 30th Int. Cosmic Ray Conf.*, ed. R. Caballero, J. C. D'Olivo, G. Medina-Tanco, L. Nellen, F. A. Sanchez, & J. F. Valdes-Galicia, Vol. 3, 1175
- [13] Mastichiadis, A., & Kazanas, D. 2009, *ApJ*, 694, L54
- [14] Norris, J. P., Marani, G. F., & Bonnell, J. T. 2000, *ApJ*, 534, 248
- [15] Norris, J. P. 2002, *ApJ*, 579, 386
- [16] Nousek, J. A. et al. 2000, *ApJ*, 642, 389
- [17] Petropoulou, M., Mastichiadis, A., & Piran, T. 2011, *A&A*, A76
- [18] Racusing, J. L. et al. 2009, *ApJ*, 698, 43
- [19] Racusing, J. L. et al. 2011, *ApJ*, 738, 138
- [20] Rees, M. J., & Mészáros, P. 1992, *MNRAS*, 258, 41
- [21] Sari, R., Piran, T., & Narayan, R. 1998, *ApJ*, 497, L17
- [22] Sari, R., Piran, T., & Halpern, J. P. 1999, *ApJ*, 519, L17
- [23] Schaefer, B. E. 2007, *ApJ*, 660, 16
- [24] Shen, R., & Matzner C. D. 2012, *ApJ*, 744, 36
- [25] Sultana, J., Kazanas, D., & Mastichiadis, A. 2013, *ApJ*, 779, 16
- [26] Sultana, J., Kazanas, D., & Fukumura, K. 2012, *ApJ*, 758, 32
- [27] Tagliaferri, G., et al. 2005, *Nature*, 436, 985
- [28] Wang, F.-Y., Qi, S. & Dai, Z.-G. 2011, *MNRAS*, 415, 3423
- [29] Willingale, R., & O'Brien, P. T. 2007, *Phil. Tran. R. Soc. A*, 365, 1179
- [30] Zhang, B. et al. 2006, *ApJ*, 642, 354
- [31] Zhang, B. 2007, *Chin. J. As. Ap.* 2007, 7, 1